doi:10.1016/j.jmb.2008.11.009 J. Mol. Biol. (2009) 385, 1257–1265

JMB

Available online at www.sciencedirect.com

ScienceDirect

ELSEVIER

A New Amyloid-Like β-Aggregate with Amyloid Characteristics, Except Fibril Morphology

Evan S.-H. Chang[1], Tai-Yan Liao[1], Tsong-Shin Lim[3], Wunshain Fann[2] and Rita P.-Y. Chen[1]*

[1]*Institute of Biological Chemistry, Academia Sinica, No. 128, Sec 2, Academia Road, Nankang, Taipei 115, Taiwan, ROC*

[2]*Institute of Atomic and Molecular Sciences, Academia Sinica, Taipei 115, Taiwan, ROC*

[3]*Department of Physics, Tunghai University, Taichung 407, Taiwan, ROC*

Received 3 June 2008; received in revised form 6 November 2008; accepted 10 November 2008
Available online 18 November 2008

Edited by J. Weissman

Amyloid plaques, formed from amyloid β (Aβ) peptides (mainly Aβ40 or Aβ42), are one of the most important pathological characteristics of Alzheimer's disease. Here, a single D-form proline substitution in the 40-amino-acid Aβ40 peptide can totally change the aggregation behavior of this peptide. The residue immediately preceding each glycine in Aβ40 (S8, V24, I32, and V36) was individually replaced by D-form proline (^{D}Pro). The resulting ^{D}P-G sequence (the ^{D}Pro residue and the following Gly residue) was designed as a "structural clip" to force the formation of a bend in the peptide, as this sequence has been reported to be a strong promoter of β-hairpin formation. The mutant peptide with Val24-to-^{D}Pro substitution, named V24P, formed a new amyloid-like β-aggregate at high peptide concentration. The aggregate has most of the characteristics of amyloid fibrils, except fibril morphology. Moreover, the mutant peptide V24P, when mixed with Aβ40, can attenuate the cytotoxicity of Aβ40.

Keywords: amyloid; fibril; aggregate; Alzheimer; Aβ

Introduction

The structural properties of the major cleaved products of amyloid precursor protein (APP)—amyloid β (Aβ) 40 and Aβ42, as very likely culprits of Alzheimer's disease—have been studied extensively by examining the behavior of mutant peptides with various lengths,[1–4] modifications,[5,6] and substitutions.[7–15] A structural model for Aβ40 amyloid has been proposed.[16] Residues 25–29 contain a bend that brings the two β-strands formed from residues 12–24 (β1) and residues 30–40 (β2) in close contact through interactions between side chains. Each β-strand forms a parallel β-sheet by forming hydrogen bonds with the same strand of another molecule. On the surface of these two β-sheets, the side chains of these residues form ridges, and the spaces between them form grooves. Sheet-to-sheet packing is stabilized by complementary fitting of these ridges and grooves. However, this packing arrangement is not absolute. In the structural model of Aβ42 amyloid,[17] parallel β-sheets are formed from residues 18 to 26 (β1) and from residues 31 to 42 (β2), but a two-residue extension at the C-terminus shifts the packing by three residues toward the C-terminal end. (It should be noted that Met35 of Aβ42 is oxidized in this study. Whether the modification affects the resulting amyloid structure remains elusive.)[17] The different packing arrangement indicates the structural plasticity of Aβ peptides. Here, we attempted to create an artificial bend at different positions in the Aβ40 peptide to examine whether the bend on the polypeptide chain can alter the amyloidogenic property of the peptide. The ^{D}Pro-Gly sequence has a high structural proclivity to populate a type II′ β-turn, which favors the formation of a left-handed β-hairpin,[18–23] and D-form proline has been widely used in designed peptide sequences to form a β-structure. In the amino acid sequence of Aβ40, Ser8, Val24, Lys28, Ile32, and Val36 are followed by a glycine residue. Each of these was individually replaced with a D-form proline to

**Corresponding author.* E-mail address: pyc@gate.sinica.edu.tw.

Abbreviations used: Aβ, amyloid β; APP, amyloid precursor protein; ThT, thioflavin T; CR, Congo red; PBS, phosphate-buffered saline; MTT, 3-[4,5-dimethylthiazol-2-yl]-2,5-diphenyltetrazolium bromide.

create a bend. The mutated peptides were respectively named S8P, V24P, K28P, I32P, and V36P, and, with the exception of K28P, were prepared by solid-phase peptide synthesis. The effects of this introduced backbone bending on the amyloidogenic property of these peptides were then studied.

Results

Structural conversions of mutated peptides

K28P proved difficult to synthesize. Peptides S8P, V24P, I32P, and V36P were synthesized and compared with the wild-type Aβ40 peptide to examine the effect of the introduced bend on amyloid formation by the peptide. Characterized by the formation of a cross-β structure, amyloid formation can be detected and quantified by various spectroscopic techniques:[24] the appearance of negative ellipticity at 218 nm can be detected by circular dichroism (CD) spectroscopy;[25] emitted fluorescence intensity at 487 nm upon binding to thioflavin T (ThT) can be detected by fluorescence spectroscopy;[26–28] an increased absorption peak at ~1628 cm^{-1} can be detected by Fourier transform infrared spectroscopy[24,29] an increased and red-shifted absorption peak can be detected by absorption spectroscopy; birefringence under polarized light upon binding to Congo red (CR) can be detected by optical microscopy[30,31] aggregate-induced light scattering can be detected by spectrofluorometry;[32] and fibril morphology can be detected by electron microscopy and atomic force microscopy. The effects of the ^{D}Pro substitution on the amyloidogenic property of Aβ40 were first examined by CD spectroscopy. The ^{D}P-G bend in peptide S8P did not inhibit amyloid formation by the peptide. This is not surprising as, based on the previously published structural model,[16] Ser8 is in the flexible region outside the amyloid core. However, the mutations in the C-terminal part of the peptide had a profound effect. The peptide V24P remained as a random coil structure at a peptide concentration as high as 30 μM (Fig. 1b) and formed a β-sheet structure when the peptide concentration was increased (Fig. 1a). Moreover, this β-sheet formation was very rapid without lag time (Fig. 1c). For 60 μM V24P, the CD spectra showed no difference at different incubation times. The thermodynamic solubility of the peptide was largely increased. By measuring the peptide concentration in the soluble portion after centrifugation, the thermodynamic solubility of Aβ40, S8P, and V24P is determined as 3.48±0.30, 4.52±0.25, and 29.44±0.26 μM, respectively. Apparently, the substitution V24→^{D}P largely increased peptide solubility. This effect is not only due to the removal of the hydrophobic side chain of Val24 but also contributed by the special configuration of D-form proline. Williams *et al.* have measured the critical concentrations of various Aβ40 mutants with the L-form Pro substitution at different positions.[7] The V24→^{L}P substitution also increased

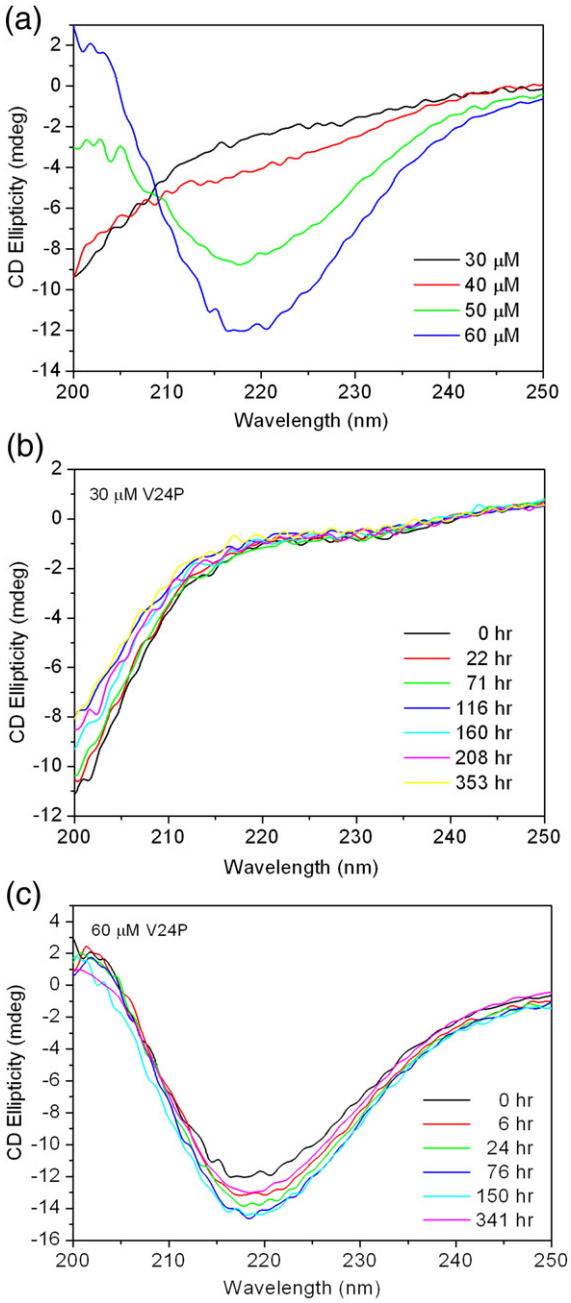

Fig. 1. Concentration-dependent coil-to-β structural conversion of V24P. (a) V24P was dissolved in 20 mM sodium phosphate buffer and 150 mM KCl (pH 7) at a concentration of 30, 40, 50, or 60 μM (black, red, green, and blue lines, respectively), and the CD spectrum was recorded immediately. CD spectra of 30 μM (b) and 60 μM (c) V24P at different incubation times.

the critical concentration from 0.9 to 8 μM. (It should be noted that the critical concentration of wild-type Aβ40 in their measurement is lower than the solubility in our measurement. They used higher centrifugation speed and quantified the concentration by reverse-phase HPLC.) The D-form Pro substitution in our study increased the peptide solubility more greatly than the L-form Pro, suggesting that the ^{D}Pro-Gly sequence has a more profound effect than

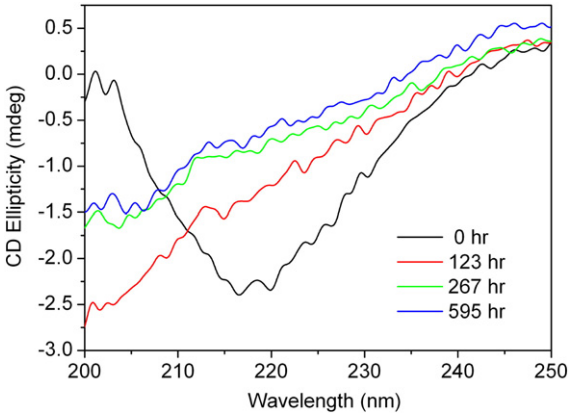

Fig. 2. Reversibility of the structural conversion of the β-structure formed by the V24P peptide. CD spectra of V24P β-structures after threefold dilution. The V24P peptide was dissolved in 20 mM sodium phosphate buffer with 150 mM KCl (pH 7) at a peptide concentration of 50 μM. The solution was incubated at room temperature for 20–30 days and then was diluted with 2 vol of the same buffer. The CD spectra of the solution after dilution were recorded at different times.

the ^{L}Pro-Gly sequence on the stabilization of the monomer structure.

The β-structure formed from the mutated peptide V24P was unstable and very sensitive to peptide concentration. When the 50 μM V24P solution was diluted threefold with the same buffer, the intensity of the negative CD ellipticity at 218 nm decreased, and a slow transformation into a random coil structure was observed (Fig. 2). After dilution, the final peptide concentration (16.7 μM) was lower than the thermodynamic solubility of the V24P peptide (29.44 μM). Therefore, the β-aggregate was redissolved and converted back to random coil.

Surprisingly, the aggregate formed from the V24P peptide did not show fibril morphology under an electron microscope (Fig. 3). Only amorphous aggregate was found. However, this structure was able to bind various dyes that are often used in amyloid quantification, such as ThT and CR. Moreover, apple green birefringence can be observed for the aggregate placed under polarized light (Fig. 4). As shown in Fig. 5, at a concentration of 30 μM, V24P did not show ThT fluorescence, as expected from the random coil structure seen in the CD spectrum (Fig. 1a), whereas 60 μM V24P emitted high fluorescence when bound to ThT as the amyloid fibrils formed from Aβ40 and S8P.

In the CR binding assay, a 30 μM V24P solution behaved similarly to a wild-type Aβ40 monomer (peptide sample without incubation before measurement) and the buffer control, with no absorption increase observed when mixed with CR (Fig. 6a). In contrast, the 60 μM V24P solution showed a high absorption increase and red shift of the absorption peak, suggesting that the β-structure formed at a high concentration of V24P has a high affinity for CR. However, the shape of the difference spectrum was distinguishable from those of amyloid fibrils formed from wild-type Aβ40 and mouse prion peptide 108–144, which was used as positive control. In Fig. 6b, the 60 μM V24P solution showed a maximum at 524 nm, while the other two had a maximum at 535 nm. The CR binding assay is less sensitive than the ThT binding assay to amyloid quantification because the absorption increase is not as large as the ThT fluorescence increase. However, based on our results, the CR binding assay has the advantage of distinguishing between different β-sheet-rich assemblies.

I32P and V36P showed behaviors similar to those of V24P, except that a higher peptide concentration was required for the structural conversion (data not shown). Therefore, in this study, we only focus on V24P.

Comparison of Aβ amyloid fibrils and the β-aggregate formed from V24P

ThT fluorescence, CR-binding ability, and birefringence suggested that the β-structure formed from V24P has amyloid characteristics. However, the absence of fibril morphology suggested that the coil-to-β structural conversion shown in the CD spectra of the V24P peptide did not come from a typical amyloid fibril, but was probably due to an oligomer or polymer with a β-structure stabilized by intermolecular association. Moreover, less red shifting in the CR-binding absorption spectrum of

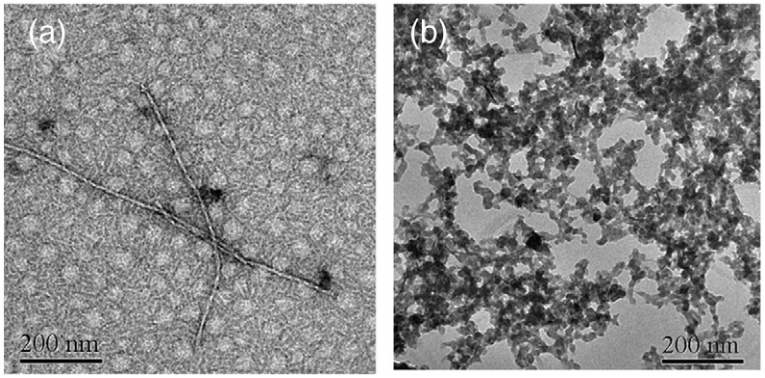

Fig. 3. Electron microscopy images of (a) Aβ40 (30 μM) and (b) V24P (60 μM).

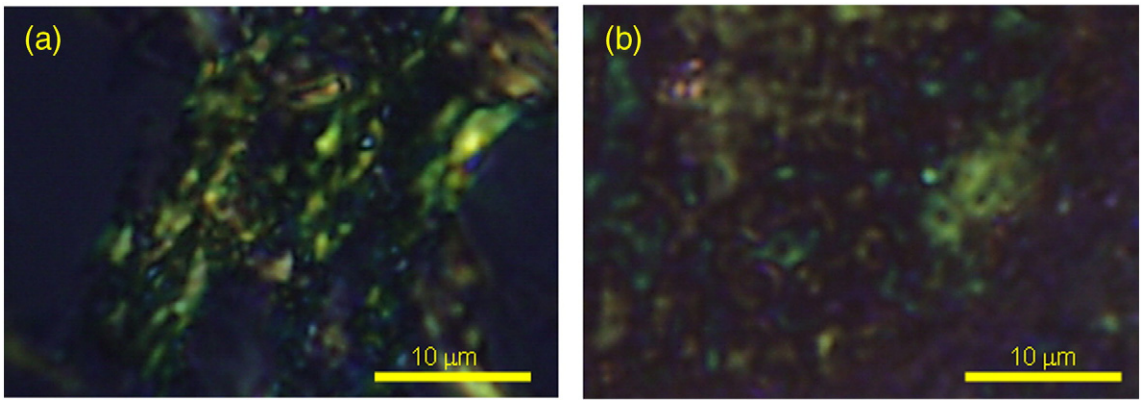

Fig. 4. Images of the aggregated (a) Aβ40 (30 μM) and (b) V24P (60 μM) under polarized light upon staining with CR.

60 μM V24P has also pointed out the structural difference between the β-amyloid fibrils and the V24P β-aggregate.

It has been proposed that the ThT fluorescence of amyloid resulted from the restricted rotation of the two rings in ThT by the hydrophobic pocket formed by the amino acid side chains of amyloid fibrils; thus, its fluorescence quantum yield is increased.[33,34] Because the lifetime of a fluorophore is sensitive to its environment, we employed a time-resolved lifetime measurement to compare the amyloid-like β-aggregate of V24P and the amyloid fibrils formed from wild-type Aβ40 and S8P. A comparison of fluorescence intensity decays is shown in Fig. 7. Using isothermal titration calorimetry, Groening *et al.* reported that there are at least two independent ThT-binding sites in the insulin fibril structure.[35] Krebs *et al.* suggested that ThT binds in the "channel" between every second residue of the two β-sheets in Aβ, with the long axis of the dye parallel with the fibril axis.[27] Based on this assumption, depending on the length of the β-strands involved in the amyloid core, there may be several binding channels. The nonlinear decay in the log plot of Fig. 7 clearly indicates that there was more than one ThT-binding channel in all these β-structures. The fluorescence decay trace of the S8P fibrils overlapped very well with that of Aβ40, confirming that these two amyloid structures have the same amyloid core and that the N-terminal part of the Aβ sequence is not involved in the amyloid core structure. In contrast, the fluorescence decay of the β-structure formed by V24P was slower, suggesting that the ThT-binding sites in this β-structure are different from those in the other two.

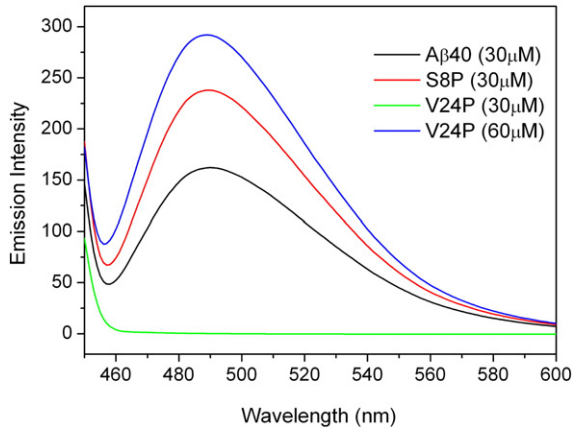

Fig. 5. ThT binding assay of V24P (30 and 60 μM), Aβ40 (30 μM), and S8P (30 μM). Peptides were dissolved in 20 mM sodium phosphate buffer and 150 mM KCl (pH 7) at the indicated concentrations and incubated before measurement.

Cytotoxicity of V24P

Is the β-aggregate formed from the peptide V24P cytotoxic? Despite their structural differences, both 30 and 60 μM V24P showed slight toxicity similar to that found in mouse N2a neuroblastoma cells ($P<0.0001$, compare with untreated cells) (Fig. 8). The data indicated that the structural conversion of V24P did not make it more toxic. Moreover, although 60 μM V24P could convert into an amyloid-like β-structure with the same ThT-binding ability as the Aβ40 fibrils, V24P was significantly less toxic than Aβ40 ($P<0.0001$). Our data indicated that the toxicity of Aβ40 might come from a special structure (probably oligomers; see Supplementary Material) and is unrelated to its amyloid characteristics. More interestingly, it seems that V24P is able to prohibit the wild-type Aβ40 from forming toxic conformers. When 30 μM Aβ40 was coincubated with 30 μM V24P, the presence of V24P attenuated the toxicity of Aβ40. We surmised that the oligomerization of the Aβ40 peptide was probably diverted by the existence of V24P.

Discussion

The origin of the term "amyloid" comes from the spectroscopic properties of a proteinaceous aggregate similar to those of starch (amylose). CR and ThT binding assays have been widely used in amyloid identification. There has been some suspicion that the dye binding assay does not necessarily provide a quantitative measurement of fibril formation,[24,32,36] and this was substantiated by our results. Our results

demonstrated that an amorphous aggregate can possibly be formed and possibly contributed to the observed ThT fluorescence and CR absorption signals. Since fibril morphology is generally considered as a requisite for the protein aggregate to be described as amyloid, we call our V24P aggregate an amyloid-like β-aggregate that has most of the spectroscopic characteristics of amyloids, except fibril morphology.

In the present study, we introduced an artificial bend at various positions in the Aβ40 sequence by replacing the residue in front of each glycine with a D-form proline. The introduced bend in the N-terminal part of the peptide (the S8P mutant) did not significantly affect the amyloid formation, consistent with a previous observation that the N-terminal part of the Aβ peptides is not involved in the amyloid core structure.[7,8,10,11] Accordingly, it is reasonable to assume that the S8P mutation does not affect the toxicity of the Aβ peptide (Fig. 8). In contrast, the bend introduced in the C-terminal part of the Aβ40 sequence (V24P, I32P, and V36P) largely increases the thermodynamic solubility of the peptides. Instead of forming a nucleus then amyloid fibrils, the peptides rapidly associated when the peptide concentration was higher than the threshold. The association created a kind of β-sheet-rich assembly that, similarly to amyloid fibrils, was able to bind CR and ThT. The high ThT fluorescence intensity for the 60 μM V24P solution suggested that ThT assay does not necessarily provide a reliable quantitative measure of fibril formation. We propose that the ^{D}P-G sequence at residues 24 and 25 might induce a bend in the middle of the peptide. However, one tight turn is not enough to support β-hairpin formation. The β-structure is stabilized by further intermolecular association, which is dependent on

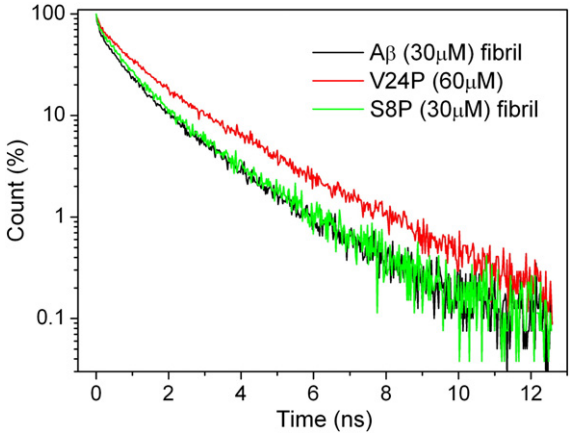

Fig. 7. Time-dependent intensity decay of ThT bound to Aβ40 fibrils (black), S8P fibrils (green), or V24P aggregates (red).

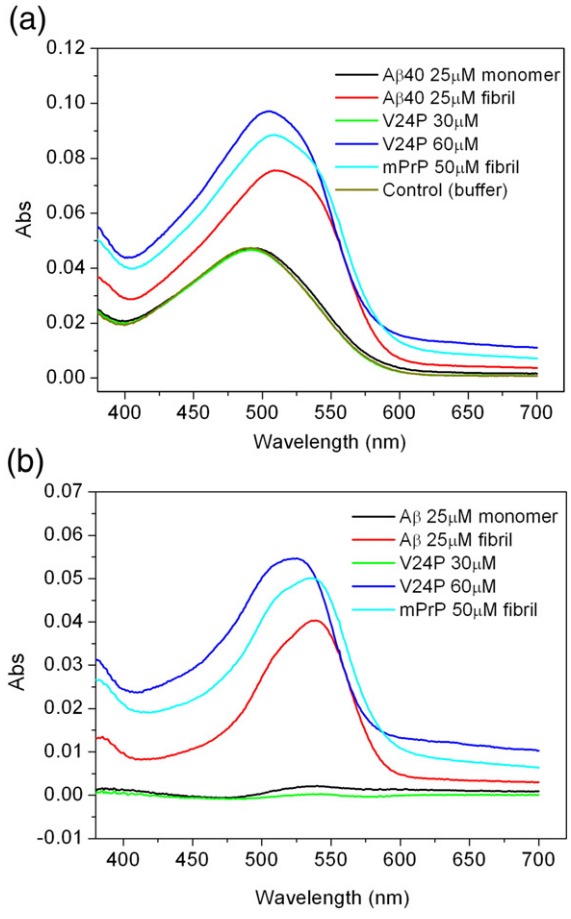

Fig. 6. CR binding assay. (a) Absorption spectra after CR binding to 25 μM Aβ40 monomer solution (black), 25 μM Aβ40 fibril solution (red), 30 μM V24P solution (green), and 60 μM V24P solution (blue). Amyloid fibrils formed from mouse prion peptide (108–144) were used as positive control (cyan). The negative control of CR in the buffer is shown in orange. (b) Difference spectra from (a). The buffer spectrum was subtracted from the sample spectra.

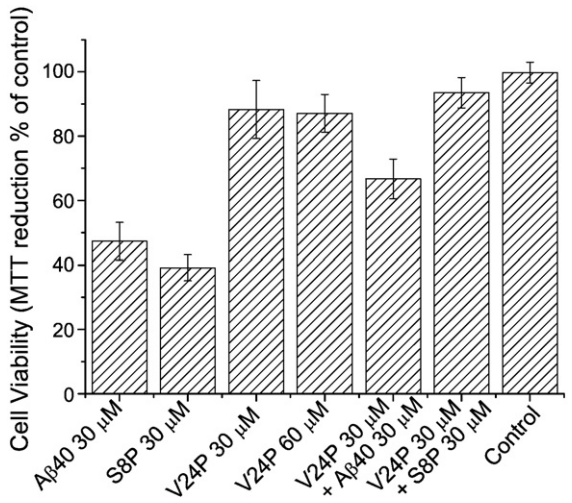

Fig. 8. Comparison of the cytotoxicities of Aβ40, S8P, and V24P. V24P (30 or 60 μM), S8P (30 μM), and Aβ40 (30 μM) were incubated at room temperature with gentle shaking for 24 h then added to the cells, and cytotoxicity was measured using MTT. Standard errors of the mean are shown as bars for each sample.

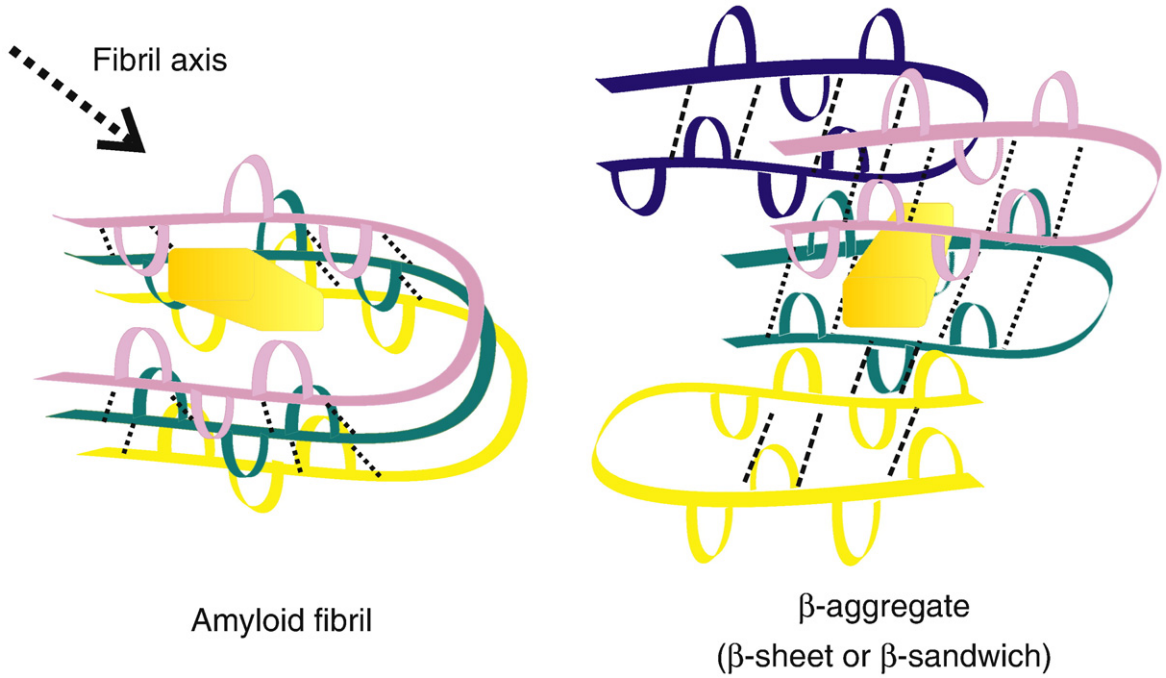

Fig. 9. Illustration of proposed ThT binding modes for Aβ amyloid fibrils (left) and the β-aggregate formed from V24P (right). The fibril elongation direction of Aβ amyloid fibrils is shown by an arrow. Each monomer is colored differently. Hydrogen bonds are expressed as black dotted lines. ThT molecule is presented as a yellow block.

the peptide concentration. The resulting V24P β-aggregate still has hydrophobic channels for ThT binding. The proposed ThT binding mode in the proposed V24P β-aggregate structure is shown in Fig. 9. However, its side-chain pairing is different from that in Aβ40 fibrils, as reflected in the difference in ThT fluorescence lifetimes. Moreover, the less red shift observed in the CR-binding absorption spectrum of 60 μM V24P also suggested that these two β-rich structures are different.

Why can a single ^{D}Pro substitution have such a dramatic effect on the structural property of the Aβ40 peptide? In the structural model of Aβ40,[16] the two β-strands of the peptide are separated by a 180° bend formed by residues 25–29. Due to its special configuration, ^{D}Pro has a ϕ-angle of +60°. Compared with ^{L}Pro, which also has a rigid ring structure, the positive ϕ-angle of ^{D}Pro is able to direct the polypeptide chain to the opposite direction. We suggest that this new bend of V24P inhibits nucleus packing and subsequent amyloid fibril formation, and largely increases the solubility of the peptide in aqueous solution.

In the last decade, the identification of an Aβ oligomer and its cytotoxicity[37,38] initiated the discussion of multiple pathways involved in the aggregation of Aβ peptides.[9] The population of Aβ peptides following different pathways, including the formation of spherical oligomers, worm-like protofibrils, or mature fibrils, depends on the plastic nature of the peptides in the environment.[9,39–42] Our findings reinforced the structural plasticity of the C-terminal part of the Aβ peptide. With one single ^{D}Pro substitution functioning as a "structural clip," the bending in the C-terminal part of the Aβ peptide clearly changes the structural propensity of the peptide. Whether or not forming the amyloid-like aggregate, the mutant peptide V24P is less toxic than the wild-type peptide in the cell viability assay. More interestingly, when coincubated with Aβ40, the cytotoxicity of Aβ40 is decreased. We surmise that V24P, with the same hydrophobic segment as Aβ40, might associate with Aβ40 and prohibit the formation of toxic oligomers. Based on the amyloid hypothesis, the targets for amyloid-related therapy of Alzheimer's disease include the following: (1) reduction of APP expression;[43] (2) alteration of APP processing[44,45] (3) inhibition and reversion of Aβ aggregation;[46] and (4) clearance of Aβ peptides or plaques.[47] We proposed that designing a peptide that is able to "trap" Aβ peptides or to divert the misfolding pathway of the Aβ peptides might be another strategy in the therapy of Alzheimer's disease.

Materials and Methods

Peptide synthesis

The peptides were prepared by the batch Fmoc polyamide method.[22] After deprotection and purification, they were characterized by mass spectroscopy, lyophilized, and stored at −20 °C.

CD spectroscopy

The peptides were dissolved at the indicated concentration in 20 mM sodium phosphate buffer and 150 mM KCl (pH 7), and the solution was incubated at room temperature. After different incubation times, the samples

were placed in a 1-mm cell, and CD spectra between 200 and 250 nm were recorded on a J-715 CD spectrometer (JASCO, Japan). The bandwidth was set to 2 nm, and the step resolution was 0.05 nm. Two scans were averaged for each sample.

ThT binding assay

A stock solution of 2 mM ThT was prepared in 140 mM KCl and 100 mM sodium phosphate buffer (pH 7.5), and filtered through a 0.22-μm Millipore filter. A fresh working solution was prepared by adjusting the dye concentration to 200 μM. A 30-μL aliquot of the sample was mixed with 30 μL of a 200 μM ThT dye solution for 1 min at room temperature, then the fluorescence emission between 450 and 600 nm was measured in a 3-mm-pathlength rectangular cuvette on a FP-750 spectrofluorometer (JASCO) with excitation at 442 nm.

CR binding assay

A 2 mM CR stock solution was prepared in 150 mM NaCl and 5 mM potassium phosphate buffer (pH 7.4) with continuous stirring and was passed through a 0.22-μm Millipore filter. A fresh working solution was prepared by adjusting the dye concentration to 200 μM. A 30-μL aliquot of the sample was mixed with 2 μL of 200 μM CR and 120 μL of the above buffer for 15 min at room temperature, then the UV spectrum between 380 and 700 nm was recorded on a DU 800 spectrophotometer (Beckman, USA). The difference spectrum was obtained by subtracting the control spectrum from the sample spectrum.

Electron microscopy

Solutions of Aβ40 (30 μM) and V24P (60 μM) in 20 mM sodium phosphate buffer (pH 7) containing 150 mM KCl were incubated at room temperature until a β-structure had been found by CD spectroscopy. Negative staining was performed on formvar- and carbon-coated 300-mesh copper grids. The samples were loaded onto the grid, left for 3 min for absorption, and then stained with 2% uranyl acetate for 40 s. Extra dye was washed away with water. After overnight drying in a desiccator, the samples were viewed on a JEM-2011 electron microscope (JEOL, Japan) at 200 kV.

CR birefringence assay

Twenty microliters of the CR working solution was added into 200 μL of the aggregated Aβ40 (30 μM) or V24P (60 μM) solution, and the mixture was incubated for 1 day. The solution was centrifuged at 15,000*g* for 10 min to isolate the aggregates. The aggregated pellet was resuspended in 30 μL of deionized water. Ten microliters of the suspended solution was loaded onto a glass microscopy slide and air-dried. The sample was examined using polarized light microscopy (Olympus BX50 equipped with a U-POT polarizer and a U-ANT analyzer).

Determination of thermodynamic solubility by amino acid composition analysis

Solutions of Aβ40 (30 μM), S8P (30 μM), and V24P (60 μM) in 20 mM sodium phosphate buffer (pH 7) containing 150 mM KCl were incubated at room temperature until the structural conversion had reached equilibrium. The amyloid fibrils and aggregates were separated from the remaining monomer solution by centrifugation at 16,000*g* for 20 min. Two hundred fifty microliters of the monomer solutions was carefully taken out. Fifteen microliters of 600 μM norvaline was added as internal standard. Finally, 1.59 mL of HCl/TFA (4:1) solution was added. The final mixture was placed into the hydrolysis tube. After being filled with nitrogen, the hydrolysis tube was heated at 143 °C for 3 h. The hydrolyzed solution was lyophilized to remove acid. The powder was redissolved in 30 μL of 0.1 N HCl. Amino acid composition was determined using the Agilent ZORBAX Eclipse AAA kit.

Fluorescence lifetime measurement

A 30 μM solution of Aβ40 in 20 mM sodium phosphate buffer (pH 7) containing 150 mM KCl was incubated at room temperature until amyloidogenesis had reached equilibrium, then the sample was centrifuged at 14,000*g* for 10 min at room temperature to remove the peptide monomer, and the fibrils were suspended in the same volume of buffer. A sample (100 μL) of the Aβ40 fibril suspension was mixed with 10 μL of 200 μM ThT dye to measure fluorescence lifetimes. In the case of V24P, 10 μL of a 200 μM ThT solution was added to 100 μL of the 60 μM V24P peptide solution immediately before measurement. A mode-locked tunable Ti:sapphire laser (Mira 900 operating at $\lambda =$ 880 nm, 76 MHz pulse rate, and 200 fs pulse width; Coherent) was passed through a second harmonic generator to generate a 440-nm-wavelength light as excitation source. The emitted light was passed through a bandpass filter (center wavelength, 480 nm; bandwidth, 30 nm) and a double-grating monochromator operating at 480 nm, and detected by a photomultiplier tube. Part of the laser pulse was directed to a silicon photodiode, which acted as reference signal. The time interval between the fluorescence signal and the reference signal was used to construct the fluorescence decay curves.

Cell viability assay

Mouse N2a neuroblastoma cells (ATCC) were cultured in Dulbecco's modified Eagle's medium (DMEM) (HyClone, USA) supplemented with 10% fetal bovine serum (HyClone) in 5% CO_2 at 37 °C. For cell viability assay, the cells were harvested and suspended at a density of 350,000 cells/mL in DMEM, and 100 μL was plated in each well of a 96-well CellBIND polystyrene microplate (Corning, USA). Because the cytotoxicity experiments lasted up to 4 days, cell proliferation was blocked using a medium with no fetal bovine serum. The plates were then incubated at 37 °C under 5% CO_2 for 24 h to allow the cells to attach. The wild-type Aβ40, S8P, and V24P peptides were dissolved in DMSO as 6 and 12 mM stock solutions. Five microliters of the stock solution was diluted with 95 μL of phosphate-buffered saline (PBS; 20 mM sodium phosphate buffer and 150 mM KCl, pH 7.0), then the sample was immediately added to 900 μL of fresh DMEM medium to give a peptide concentration of 30 or 60 μM. To make a mixture of Aβ40 and V24P peptides, equal volumes of 12 mM Aβ40 and V24P stock solution were premixed and then diluted into PBS to make a final concentration of 30 μM for each peptide. The mixture of S8P and V24P peptides was prepared in the same way. The diluted peptide solutions were preincubated for 24 h at room temperature with shaking (50 rpm) before being

added to the cultures. The medium in the well of the 96-well plate was replaced with 100 μL of peptide-containing medium, and the plate was incubated for 48 h, then cell viability was determined using the 3-[4,5-dimethylthiazol-2-yl]-2,5-diphenyltetrazolium bromide (MTT) toxicity assay.[48] Ten microliters of 5 mg/mL MTT in PBS was added to each well. After incubation for 4 h, the medium was removed, and the MTT crystals were dissolved in 100 μL of 90% isopropanol, 0.5% SDS, and 40 mM HCl, and the absorption at 570 nm was measured and background-corrected. Cell viability was calculated by dividing the corrected absorbance of wells containing peptide samples by that of wells without any added peptide, and then expressed as a percentage of the value with no added peptide. The average of 16 replicate wells was used for each sample and control, and the experiment was repeated at least three times.

Acknowledgements

We thank Dr. Wei-Hau Chang (Institute of Chemistry), Ms. Yao-Yin Chuang (Institute of Chemistry), and Ms. An-Li Huang (Institute of Biomedical Sciences, Academia Sinica) for their kind help with electron microscopy. We also acknowledge Dr. Huei-Chun Chang (Biophysical Instrumentation Laboratory, Institute of Biological Chemistry) for technical support and Dr. Chien-Chih Yang (Department of Biochemical Science and Technology, National Taiwan University) for his kind help with the recording of CR birefringence images.

Supplementary Data

Supplementary data associated with this article can be found, in the online version, at doi:10.1016/j.jmb.2008.11.009

References

1. Liu, R., McAllister, C., Lyubchenko, Y. & Sierks, M. R. (2004). Residues 17–20 and 30–35 of β-amyloid play critical roles in aggregation. *J. Neurosci. Res.* **75**, 162–171.
2. Soto, C., Kindy, M. S., Baumann, M. & Frangione, B. (1996). Inhibition of Alzheimer's amyloidosis by peptides that prevent β-sheet conformation. *Biochem. Biophys. Res. Commun.* **226**, 672–680.
3. Lin, S. Y. & Chu, H. L. (2003). Fourier transform infrared spectroscopy used to evidence the prevention of beta-sheet formation of amyloid β(1–40) peptide by a short amyloid fragment. *Int. J. Biol. Macromol.* **32**, 173–177.
4. Ban, T., Hoshino, M., Takahashi, S., Hamada, D., Hasegawa, K., Naiki, H. & Goto, Y. (2004). Direct observation of Aβ amyloid fibril growth and inhibition. *J. Mol. Biol.* **344**, 757–767.
5. Schilling, S., Lauber, T., Schaupp, M., Manhart, S., Scheel, E., Bohm, G. & Demuth, H. U. (2006). On the seeding and oligomerization of pGlu-amyloid peptides (*in vitro*). *Biochemistry*, **45**, 12393–12399.
6. Johansson, A. S., Bergquist, J., Volbracht, C., Paivio, A., Leist, M., Lannfelt, L. & Westlind-Danielsson, A. (2007). Attenuated amyloid-β aggregation and neurotoxicity owing to methionine oxidation. *NeuroReport*, **18**, 559–563.
7. Williams, A. D., Portelius, E., Kheterpal, I., Guo, J. T., Cook, K. D., Xu, Y. & Wetzel, R. (2004). Mapping Aβ amyloid fibril secondary structure using scanning proline mutagenesis. *J. Mol. Biol.* **335**, 833–842.
8. Morimoto, A., Irie, K., Murakami, K., Masuda, Y., Ohigashi, H., Nagao, M. *et al.* (2004). Analysis of the secondary structure of β-amyloid (Aβ42) fibrils by systematic proline replacement. *J. Biol. Chem.* **279**, 52781–52788.
9. Wetzel, R., Shivaprasad, S. & Williams, A. D. (2007). Plasticity of amyloid fibrils. *Biochemistry*, **46**, 1–10.
10. Wood, S. J., Wetzel, R., Martin, J. D. & Hurle, M. R. (1995). Prolines and amyloidogenicity in fragments of the Alzheimer's peptide β/A4. *Biochemistry*, **34**, 724–730.
11. Williams, A. D., Shivaprasad, S. & Wetzel, R. (2006). Alanine scanning mutagenesis of Aβ(1–40) amyloid fibril stability. *J. Mol. Biol.* **357**, 1283–1294.
12. Kim, W. & Hecht, M. H. (2006). Generic hydrophobic residues are sufficient to promote aggregation of the Alzheimer's Aβ42 peptide. *Proc. Natl Acad. Sci. USA*, **103**, 15824–15829.
13. Kim, W. & Hecht, M. H. (2005). Sequence determinants of enhanced amyloidogenicity of Alzheimer Aβ42 peptide relative to Aβ40. *J. Biol. Chem.* **280**, 35069–35076.
14. Shanmugam, G., Polavarapu, P. L., Hallgas, B. & Majer, Z. (2005). Effect of D-amino acids at Asp23 and Ser26 residues on the conformational preference of Aβ20–29 peptides. *Biochem. Biophys. Res. Commun.* **335**, 712–722.
15. Kaneko, I., Morimoto, K. & Kubo, T. (2001). Drastic neuronal loss *in vivo* by beta-amyloid racemized at Ser(26) residue: conversion of non-toxic [D-Ser(26)]β-amyloid 1–40 to toxic and proteinase-resistant fragments. *Neuroscience*, **104**, 1003–1011.
16. Petkova, A. T., Ishii, Y., Balbach, J. J., Antzutkin, O. N., Leapman, R. D., Delaglio, F. & Tycko, R. (2002). A structural model for Alzheimer's β-amyloid fibrils based on experimental constraints from solid state NMR. *Proc. Natl Acad. Sci. USA*, **99**, 16742–16747.
17. Luhrs, T., Ritter, C., Adrian, M., Riek-Loher, D., Bohrmann, B., Dobeli, H. *et al.* (2005). 3D structure of Alzheimer's amyloid-β(1–42) fibrils. *Proc. Natl Acad. Sci. USA*, **102**, 17342–17347.
18. Sibanda, B. L. & Thornton, J. M. (1985). Beta-hairpin families in globular proteins. *Nature*, **316**, 170–174.
19. Haque, T. S. & Gellman, S. H. (1997). Insights on beta-hairpin stability in aqueous solution from peptides with enforced type I′ and type II′ beta-turns. *J. Am. Chem. Soc.* **119**, 2303–2304.
20. Schenck, H. L. & Gellman, S. H. (1998). Use of a designed triple-stranded antiparallel beta-sheet to probe beta-sheet cooperativity in aqueous solution. *J. Am. Chem. Soc.* **120**, 4869–4870.
21. Stanger, H. E. & Gellman, S. H. (1998). Rules for antiparallel beta-sheet design: D-Pro-Gly is superior to L-Asn-Gly for beta-hairpin nucleation. *J. Am. Chem. Soc.* **120**, 4236–4237.
22. Chen, P. Y., Lin, C. K., Lee, C. T., Jan, H. & Chan, S. I. (2001). Effects of turn residues in directing the formation of the β-sheet and in the stability of the β-sheet. *Protein Sci.* **10**, 1794–1800.

23. Chen, R. P. Y., Huang, J. J. T., Chen, H. L., Jan, H., Velusamy, M., Lee, C. T. *et al.* (2004). Measuring the refolding of beta-sheets with different turn sequences on a nanosecond time scale. *Proc. Natl Acad. Sci. USA*, **101**, 7305–7310.
24. Nilsson, M. R. (2004). Techniques to study amyloid fibril formation *in vitro*. *Methods*, **34**, 151–160.
25. Chen, P. Y., Lin, C. C., Chang, Y. T., Lin, S. C. & Chan, S. I. (2002). One O-linked sugar can affect the coil-to-β structural transition of the prion peptide. *Proc. Natl Acad. Sci. USA*, **99**, 12633–12638.
26. Khurana, R., Coleman, C., Ionescu-Zanetti, C., Carter, S. A., Krishna, V., Grover, R. K. *et al.* (2005). Mechanism of thioflavin T binding to amyloid fibrils. *J. Struct. Biol.* **151**, 229–238.
27. Krebs, M. R. H., Bromley, E. H. C. & Donald, A. M. (2005). The binding of thioflavin-T to amyloid fibrils: localisation and implications. *J. Struct. Biol.* **149**, 30–37.
28. LeVine, H., III (1993). Thioflavin T interaction with synthetic Alzheimer's disease beta-amyloid peptides: detection of amyloid aggregation in solution. *Protein Sci.* **2**, 404–410.
29. Jones, E. M. & Surewicz, W. K. (2005). Fibril conformation as the basis of species- and strain-dependent seeding specificity of mammalian prion amyloids. *Cell*, **121**, 63–72.
30. Klunk, W. E., Jacob, R. F. & Mason, R. P. (1999). Quantifying amyloid by Congo red spectral shift assay. *Methods Enzymol.* **309**, 285–305.
31. Klunk, W. E., Jacob, R. F. & Mason, R. P. (1999). Quantifying amyloid beta-peptide (Abeta) aggregation using the Congo red-Abeta (CR-Abeta) spectrophotometric assay. *Anal. Biochem.* **266**, 66–76.
32. Wood, S. J., Maleeff, B., Hart, T. & Wetzel, R. (1996). Physical, morphological and functional differences between pH 5.8 and 7.4 aggregates of the Alzheimer's amyloid peptide Abeta. *J. Mol. Biol.* **256**, 870–877.
33. Groenning, M., Olsen, L., van de Weert, M., Flink, J. M., Frokjaer, S. & Jorgensen, F. S. (2007). Study on the binding of thioflavin T to beta-sheet-rich and non-beta-sheet cavities. *J. Struct. Biol.* **158**, 358–369.
34. Friedhoff, P., Schneider, A., Mandelkow, E. M. & Mandelkow, E. (1998). Rapid assembly of Alzheimer-like paired helical filaments from microtubule-associated protein tau monitored by fluorescence in solution. *Biochemistry*, **37**, 10223–10230.
35. Groenning, M., Norrman, M., Flink, J. M., van de Weert, M., Bukrinsky, J. T., Schluckebier, G. & Frokjaer, S. (2007). Binding mode of thioflavin T in insulin amyloid fibrils. *J. Struct. Biol.* **159**, 483–497.
36. Sato, T., Kienlen-Campard, P., Ahmed, M., Liu, W., Li, H., Elliott, J. I. *et al.* (2006). Inhibitors of amyloid toxicity based on beta-sheet packing of Abeta40 and Abeta42. *Biochemistry*, **45**, 5503–5516.
37. Kayed, R., Head, E., Thompson, J. L., McIntire, T. M., Milton, S. C., Cotman, C. W. & Glabe, C. G. (2003). Common structure of soluble amyloid oligomers implies common mechanism of pathogenesis. *Science*, **300**, 486–489.
38. Dahlgren, K. N., Manelli, A. M., Stine, W. B., Jr, Baker, L. K., Krafft, G. A. & LaDu, M. J. (2002). Oligomeric and fibrillar species of amyloid-beta peptides differentially affect neuronal viability. *J. Biol. Chem.* **277**, 32046–32053.
39. Bitan, G., Kirkitadze, M. D., Lomakin, A., Vollers, S. S., Benedek, G. B. & Teplow, D. B. (2003). Amyloid beta-protein (Abeta) assembly: Abeta 40 and Abeta 42 oligomerize through distinct pathways. *Proc. Natl Acad. Sci. USA*, **100**, 330–335.
40. Kodali, R. & Wetzel, R. (2007). Polymorphism in the intermediates and products of amyloid assembly. *Curr. Opin. Struct. Biol.* **17**, 48–57.
41. Stine, W. B., Jr, Dahlgren, K. N., Krafft, G. A. & LaDu, M. J. (2003). *In vitro* characterization of conditions for amyloid-beta peptide oligomerization and fibrillogenesis. *J. Biol. Chem.* **278**, 11612–11622.
42. Chen, Y. R., Huang, H. B., Chyan, C. L., Shiao, M. S., Lin, T. H. & Chen, Y. C. (2006). The effect of Abeta conformation on the metal affinity and aggregation mechanism studied by circular dichroism spectroscopy. *J. Biochem.* **139**, 733–740.
43. Shaw, K. T., Utsuki, T., Rogers, J., Yu, Q. S., Sambamurti, K., Brossi, A. *et al.* (2001). Phenserine regulates translation of β-amyloid precursor protein mRNA by a putative interleukin-1 responsive element, a target for drug development. *Proc. Natl Acad. Sci. USA*, **98**, 7605–7610.
44. Citron, M. (2000). Secretases as targets for the treatment of Alzheimer's disease. *Mol. Med. Today*, **6**, 392–397.
45. Wolfe, M. S. (2008). Gamma-secretase inhibition and modulation for Alzheimer's disease. *Curr. Alzheimer Res.* **5**, 158–164.
46. Soto, C., Sigurdsson, E. M., Morelli, L., Kumar, R. A., Castano, E. M. & Frangione, B. (1998). Beta-sheet breaker peptides inhibit fibrillogenesis in a rat brain model of amyloidosis: implications for Alzheimer's therapy. *Nat. Med.* **4**, 822–826.
47. Schenk, D., Barbour, R., Dunn, W., Gordon, G., Grajeda, H., Guido, T. *et al.* (1999). Immunization with amyloid-beta attenuates Alzheimer-disease-like pathology in the PDAPP mouse. *Nature*, **400**, 173–177.
48. Shearman, M. S., Hawtin, S. R. & Tailor, V. J. (1995). The intracellular component of cellular 3-(4,5-dimethylthiazol-2-yl)-2,5-diphenyltetrazolium bromide (MTT) reduction is specifically inhibited by beta-amyloid peptides. *J. Neurochem.* **65**, 218–227.